JOC Article

Accurate Calculation, Prediction, and Assignment of ^{3}He NMR Chemical Shifts of Helium-3-Encapsulated Fullerenes and Fullerene Derivatives

Guan-Wu Wang,*,† Xin-Hao Zhang,† Huan Zhan,† Qing-Xiang Guo,† and Yun-Dong Wu‡

Department of Chemistry, University of Science and Technology of China, Hefei, Anhui 230026, P. R. China, and Department of Chemistry, The Hong Kong University of Science and Technology, Clear Water Bay, Kowloon, Hong Kong SAR, P. R. China

gwang@ustc.edu.cn

Received January 29, 2003

Helium-3 NMR chemical shifts of various ^{3}He-encapsulated fullerenes (^{3}He@C_n) and their derivatives have been calculated at the GIAO-B3LYP/3-21G and GIAO-HF/3-21G levels with AM1 and PM3 optimized structures. A good linear relationship between the computed ^{3}He NMR chemical shifts and the experimental data has been determined. Comparisons of the calculation methods of ^{3}He NMR chemical shifts show that GIAO-B3LYP/3-21G with AM1-optimized structures yields the best results. The corrected ^{3}He NMR chemical shifts were calculated from the correction equation that is obtained through linear regression fitting of the experimental and calculated ^{3}He NMR chemical shifts over a wide range of ^{3}He-encapsulated fullerene compounds. The corrected ^{3}He NMR chemical shifts match the experimental data very well. The current computational method can serve as a prediction tool and can be applied to the assignments and reassignments of the ^{3}He NMR chemical shifts of ^{3}He@C_n and their derivatives.

Introduction

Fullerenes are quite reactive with a variety of reagents.[1−4] Most reactions result in mixtures of mono- and multiadducts. The ^{1}H NMR spectra of fullerene multiadducts generally give very complex patterns, and the structural assignments of these fullerene derivatives heavily rely on the ^{13}C NMR spectra. Because the attachment of functional groups to fullerenes lowers the high symmetry of fullerene skeletons, there are many more peaks in the ^{13}C NMR spectra of fullerene derivatives than in parent C_{60} and C_{70} spectra. It is difficult, even impossible, to assign the ^{13}C NMR peaks and, hence, the structural assignments of bis- and multi-adducts of fullerenes. Some isomers of fullerene derivatives have the same symmetry and thus give the same number of ^{13}C NMR peaks, which creates further challenges to determining the structural assignments of fullerene derivatives.

The addition of functional groups to fullerenes causes changes in the magnetic properties of fullerene skeletons. It is expected that an NMR-active nucleus placed inside a fullerene cage can sense these magnetic changes. Saunders and collaborators have prepared various ^{3}He-encapsulated fullerenes (^{3}He@C_n) and fullerene derivatives and measured their ^{3}He NMR.[5−29] Each ^{3}He@C_n and each ^{3}He@C_n derivative has a distinct chemical shift.[10] A ^{3}He NMR spectrum of a fullerene reaction mixture labeled with ^{3}He could immediately indicate how many fullerene compounds exist because all ^{3}He@C_n derivatives should show their own distinct ^{3}He NMR peaks while nonfullerene chemicals have no ^{3}He NMR peaks. Therefore, the ^{3}He NMR technique is a powerful tool to identify fullerene derivatives and to follow fullerene chemical reactions.[10] Since the successful utilization of ^{3}He NMR as a sensitive probe of the ring-current effect of ^{3}He@C_n and their derivatives, calculation of ^{3}He NMR chemical shifts has become increasingly interesting to theoretical chemists. Helium-3 NMR chemical shifts (δ_{He}) calculated at Hartree−Fock (HF) and density functional theory (DFT) levels with gauge including atomic orbitals (GIAO)

† University of Science and Technology of China.
‡ The Hong Kong University of Science and Technology.
* Corresponding author.

(1) Taylor, R.; Walton, D. R. M. *Nature* **1993**, *363*, 685−693.
(2) Hirsch, A. *Synthesis* **1995**, 895−913.
(3) Hirsch, A. *Top. Curr. Chem.* **1999**, *199*, 1−65.
(4) Thilgen C.; Diederich F. *Top. Curr. Chem.* **1999**, *199*, 135−171.
(5) Saunders, M., Jiménez-Vázquez, H. A.; Cross, R. J.; Mroczkowski, S.; Freedberg, D. I.; Anet, F. A. L. *Nature* **1994**, *367*, 256−258.
(6) Saunders, M.; Jiménez-Vázquez, H. A.; Bangerter, B. W.; Cross, R. J.; Mroczkowski, S.; Freedberg, D. I.; Anet, F. A. L. *J. Am. Chem. Soc.* **1994**, *116*, 3621−3622.
(7) Saunders, M.; Jiménez-Vázquez, H. A.; Cross, R. J.; Billups, E.; Gesenberg, C.; McCord, D. J. *Tetrahedron Lett.* **1994**, *35*, 3869−3872.
(8) Smith, A. B., III; Strongin, R. M., Brard, L.; Romanow, W. J.; Saunders, M.; Jiménez-Vázquez, H. A.; Cross, R. J. *J. Am. Chem. Soc.* **1994**, *116*, 10831−10832.
(9) Saunders, M.; Jiménez-Vázquez, H. A.; Cross, R. J.; Billups, W. E.; Gesenberg, C.; Gonzalez, A.; Luo, W.; Haddon, R. C.; Diederich, F.; Hermann, A. *J. Am. Chem. Soc.* **1995**, *117*, 9305−9308.
(10) Saunders, M.; Cross, R. J. Jiménez-Vázquez, H. A.; Shimshi, R.; Khong, A. *Science* **1996**, *271*, 1693−1697.
(11) Smith, A. B., III; Strongin, R. M.; Brard, L.; Furst, G. T.; Atkins, J. H.; Romanow, W. J.; Saunders, M.; Jiménez-Vázquez, H. A.; Owens, K. G.; Goldschmidt, R. J. *J. Org. Chem.* **1996**, *61*, 1904−1905.
(12) Schuster, D. I.; Cao, J.; Kaprinidis, N.; Wu, Y.; Jensen, A. W.; Lu, Q.; Wang, H.; Wilson, S. R. *J. Am. Chem. Soc.* **1996**, *118*, 5639−5647.
(13) Cross, R. J.; Jiménez-Vázquez, H. A.; Lu, Q.; Saunders, M.; Schuster, D. I.; Wilson, S. R.; Zhao, H. *J. Am. Chem. Soc.* **1996**, *118*, 11454−11459.

10.1021/jo0341259 CCC: $25.00
Published on Web 05/31/2003

have been performed for $^3He@C_n$ and $^3He@C_n$ derivatives.[30−40] However, the calculated δ_{He} of a given compound, e.g., $^3He@C_{60}$, varies with the calculation levels (i.e., HF or DFT) and the molecular geometries optimized at different theoretical levels. The difference between the calculated δ_{He} and the experimental δ_{He} can be as large as 6.6 ppm[31] and 11.5 ppm[32] for $^3He@C_{60}$ and $^3He@C_{70}$, respectively. The direct correlation and comparison of previously calculated chemical shifts with the experimental data might therefore lead to wrong conclusions. In this paper, we present a simple method of obtaining accurate ^{3}He NMR chemical shifts of $^3He@C_n$ and their derivatives by correlating calculated ^{3}He NMR chemical shifts with the experimental data and applying the predicted ^{3}He NMR chemical shifts to the structural assignments and reassignments of some fullerene derivatives reported in the literature.

Computational Methods

Geometries of ^{3}He-encapsulated fullerene compounds were optimized by the semiempirical methods AM1[41] and PM3.[42] Magnetic shieldings were computed at the GIAO (gauge including atomic orbitals)[43]-HF and GIAO-B3LYP (Becke's[44] three-parameter hybrid-exchange functional and the correlation functional of Lee et al.[45]) levels with the 3-21G basis set using the optimized AM1 and PM3 structures. The calculated δ_{He} are reported in ppm relative to the free ^{3}He. All calculations performed in this study were carried out with the GAUSSIAN 98 program package.[46]

Results and Discussion

The establishment of variants of the HF method with the IGLO and GIAO approaches has been a breakthrough in the field of NMR chemical shift calculations. Recently, DFT, as one of the most powerful post-HF approaches, has become a viable alternative to conventional ab initio methods. The major merit of DFT in many areas of chemistry and physics is the implicit inclusion of electron correlation effects at comparable computation costs to a HF treatment, thus allowing applications to large systems. The recent advances in ab initio methods[47] and DFT methods[38,48] in the calculation of NMR chemical shift have been reviewed.

Haddon and co-workers were the first to calculate the endohedral chemical shifts of fullerenes by the semiempirical London method. They obtained the endohedral chemical shifts of −10.1 ppm[49] and −16.8 ppm[49] for C_{60} and C_{70}, respectively. These calculated data obviously deviate from the experimental values of −6.3 ppm and −28.8 ppm for $^3He@C_{60}$ and $^3He@C_{70}$,[5] respectively. Subsequent calculations of the endohedral chemical shifts were performed at improved theoretical levels. In 1994, Cioslowski calculated the endohedral magnetic shieldings in fullerenes by ab initio GIAO−CPHF at the HF/DZP and MNDO geometries.[30,32] The calculated δ_{He} reproduced the experimental δ_{He} very well for $^3He@C_{60}$ by the GIAO-CPHF//MNDO method, but underestimated the endohedral chemical shift of $^3He@C_{70}$ for more than 11 ppm. At about the same time, Bühl and co-workers computed the δ_{He} of $^3He@C_{60}$, $^3He@C_{70}$, and $^3He@C_{60}^{6-}$ employing the GIAO-SCF method with various molecular geometries.[31] In all of the above ab initio studies, it was found that the calculated δ_{He} data were quite sensitive to geometrical changes in the fullerene structures.[30−32]

(14) Billups, W. E.; Luo, W.; Gonzalez, A.; Arguello, D.; Alemany, L. B.; Marriott, T.; Saunders, M.; Jiménez-Vázquez, H. A.; Khong, A. *Tetrahetron Lett.* **1997**, *38*, 171−174.
(15) Billups, W. E.; Gonzalez, A.; Gesenberg, C.; Luo, W.; Marriott, T.; Alemany, L. B.; Saunders, M.; Jiménez-Vázquez, H. A.; Khong, A. *Tetrahetron Lett.* **1997**, *38*, 175−178.
(16) Jensen, A. W.; Khong, A.; Saunders, M.; Wilson, S. R.; Schuster, D. I. *J. Am. Chem. Soc.* **1997**, *119*, 7303−7307.
(17) Rüttimann, M.; Haldimann, R. F.; Isaacs, L.; Diederich, F.; Khong, A.; Jiménez-Vázquez, H. A.; Cross, R. J.; Saunders, M. *Chem. Eur. J.* **1997**, *3*, 1071−1076.
(18) Khong, A.; Jiménez-Vázquez, H. A.; Saunders, M.; Cross, R. J.; Laskin, J.; Peres, T.; Lifshitz, C.; Strongin, R.; Smith, A. B., III. *J. Am. Chem. Soc.* **1998**, *120*, 6380−6383.
(19) Shabtai, E.; Weitz, A.; Haddon, R. C.; Hoffman, R. E.; Rabinovitz, M.; Khong, A.; Cross, R. J.; Saunders, M.; Cheng, P.-C.; Scott, L. T. *J. Am. Chem. Soc.* **1998**, *120*, 6389−6393.
(20) Boltalina, O. V.; Bühl, M.; Khong, A.; Saunders, M.; Street, J. M.; Taylor, R. *J. Chem. Soc., Perkin Trans. 2* **1999**, 1475−1479.
(21) Birkett, P. R.; Bühl, M.; Khong, A.; Saunders, M.; Taylor, R. *J. Chem. Soc., Perkin Trans. 2* **1999**, 2037−2039.
(22) Wilson, S. R.; Yurchenko, M. E.; Schuster, D. I.; Khong, A.; Saunders, M. *J. Org. Chem.* **2000**, *65*, 2619−2623.
(23) Wang, G.-W.; Saunders, M.; Khong, A.; Cross, R. J. *J. Am. Chem. Soc.* **2000**, *122*, 3216−3217.
(24) Wang, G.-W.; Weedon, B. R.; Meier, M. S.; Saunders, M.; Cross, R. J. *Org. Lett.* **2000**, *2*, 2241−2243.
(25) Wang, G.-W.; Saunders, M.; Cross, R. J. *J. Am. Chem. Soc.* **2001**, *123*, 256−259.
(26) Nossal, J.; Saini, R. K.; Sadana, A. K.; Bettinger, H. F.; Alemany, L. B.; Scuseria, G. E.; Billups, W. E.; Saunders, M.; Khong, A.; Weisemann, R. *J. Am. Chem. Soc.* **2001**, *123*, 8482−8495.
(27) Rubin, Y.; Jarrosson, T.; Wang, G.-W.; Bartberger, M. D.; Houk, K. N.; Schick, G.; Saunders, M.; Cross, R. J. *Angew. Chem., Int. Ed.* **2001**, *40*, 1543−1546.
(28) Fujiwara, K.; Komatsu, K.; Wang, G.-W.; Tanaka, T.; Hirata, K.; Yamamoto, K.; Saunders, M. *J. Am. Chem. Soc.* **2001**, *123*, 10715−10720.
(29) Sternfeld, T.; Hoffmann, R. E.; Saunders, M.; Cross, R. J.; Syamala, M. S.; Rabinovitz, M. *J. Am. Chem. Soc.* **2002**, *124*, 8786−8787.
(30) Cioslowski, J. *J. Am. Chem. Soc.* **1994**, *116*, 3619−3620.
(31) Bühl, M.; Thiel, W.; Jiao, H.; Schleyer, P. v. R.; Saunders, M.; Anet, F. A. L. *J. Am. Chem. Soc.* **1994**, *116*, 6005−6006.
(32) Cioslowski, J. *Chem. Phys. Lett.* **1994**, *227*, 361−364.
(33) Bühl, M.; Thiel, W. *Chem. Phys. Lett.* **1995**, *233*, 585−589.
(34) Bühl, M.; Thiel, W.; Schneider, U. *J. Am. Chem. Soc.* **1995**, *117*, 4623−4627.
(35) Bühl, M.; Wüllen, C. v. *Chem. Phys. Lett.* **1995**, *247*, 63−68.
(36) Bühl, M.; Patchkovskii, S.; Thiel, W. *Chem. Phys. Lett.* **1997**, *275*, 14−18.
(37) Bühl, M. *Chem. Eur. J.* **1998**, 4, 734−739.
(38) Bühl, M.; Kaupp, M.; Malkina, O. L.; Malkin, V. G. *J. Comput. Chem.* **1999**, *20*, 91−105.
(39) Chen, Z.; Cioslowski, J.; Rao, N.; Moncrieff, D.; Bühl, M.; Hirsch, A.; Thiel, W. *Theor. Chem. Acc.* **2001**, *106*, 364−368.
(40) Bühl, M.; Hirsch, A. *Chem. Rev.* **2001**, *101*, 1153−1183.
(41) Dewar, M. J. S.; Zoebisch, E. G.; Healy, E. F.; Stewart, J. J. P. *J. Am. Chem. Soc.* **1985**, *107*, 3902−3909.
(42) Stewart, J. J. P. *J. Comput. Chem.* **1989**, *10*, 210−264.
(43) Wolinski, K.; Hinton, J. F.; Pulay, P. *J. Am. Chem. Soc.* **1990**, *112*, 8251−8260.
(44) Becke, A. D. *J. Chem. Phys.* **1993**, *98*, 5648−5652.
(45) Lee, C.; Yang, W.; Parr, R. G. *Phys. Rev. B* **1988**, *37*, 785−789.
(46) Frisch, M. J.; Trucks, G. W.; Schlegel, H. B.; Scuseria, G. E.; Robb, M. A.; Cheeseman, J. R.; Zakrzewski, V. G.; Montgomery, J. A., Jr.; Stratmann, R. E.; Burant, J. C.; Dapprich, S.; Millam, J. M.; Daniels, A. D.; Kudin, K. N.; Strain, M. C.; Farkas, O.; Tomasi, J.; Barone, V.; Cossi, M.; Cammi, R.; Mennucci, B.; Pomelli, C.; Adamo, C.; Clifford, S.; Ochterski, J.; Petersson, G. A.; Ayala, P. Y.; Cui, Q.; Morokuma, K.; Malick, D. K.; Rabuck, A. D.; Raghavachari, K.; Foresman, J. B.; Cioslowski, J.; Ortiz, J. V.; Baboul, A. G.; Stefanov, B. B.; Liu, G.; Liashenko, A.; Piskorz, P.; Komaromi, I.; Gomperts, R.; Martin, R. L.; Fox, D. J.; Keith, T.; Al-Laham, M. A.; Peng, C. Y.; Nanayakkara, A.; Gonzalez, C.; Challacombe, M.; Gill, P. M. W.; Johnson, B.; Chen, W.; Wong, M. W.; Andres, J. L.; Gonzalez, C.; Head-Gordon, M.; Replogle, E. S.; Pople, J. A. *Gaussian* 98, Revision A.7; Gaussian, Inc.: Pittsburgh, PA, 1998.
(47) Helgaker, T.; Jaszuński, M.; Ruud, K. *Chem. Rev.* **1999**, *99*, 293−352.
(48) Schreckenbach, G.; Ziegler, T. *Theor. Chem. Acc.* **1998**, *99*, 71−82.
(49) Haddon, R. C.; Pasquarello, A. *Phys. Rev. B* **1994**, *50*, 16459−16463.

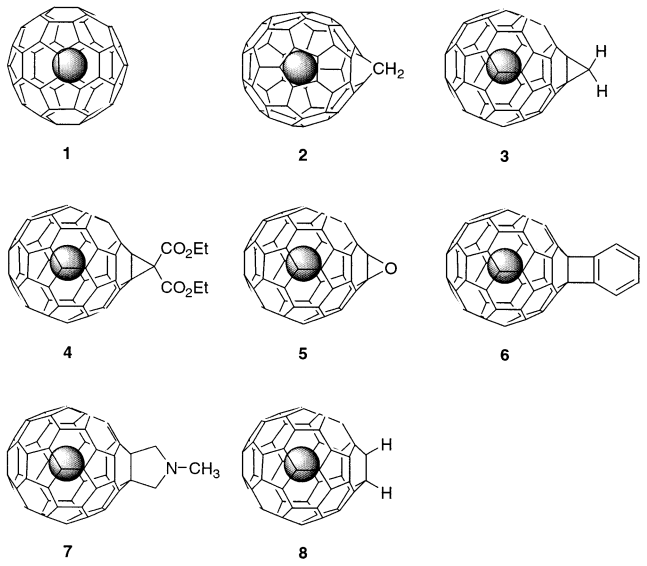

FIGURE 1. Structures of ^{3}He-encapsulated fullerene compounds **1**−**8**.

Since then, the ^{3}He NMR chemical shifts of ^{3}He@C_n and their derivatives have been calculated by the GIAO-SCF[28,33−37,39] and GIAO-DFT (UDFT-GIAO-BPW91[38] and GIAO-B3LYP[27]) methods with geometries optimized at different levels. However, there are obvious deviations between the calculated δ_{He} values and experimental δ_{He} values in all cases. Because fullerenes and fullerene derivatives are large systems, GIAO-HF/3-21G and GIAO-B3LYP/3-21G calculations with both AM1 and PM3 geometries were chosen to evaluate their validity in the ^{3}He NMR chemical shift calculations of ^{3}He@C_n and their derivatives and then to derive a method of obtaining their accurate ^{3}He NMR chemical shifts.

Comparison of the Hartree−Fock and B3LYP Methods. A series of representative ^{3}He-encapsulated fullerene compounds was selected for comparison of computation methods. These compounds were C_{60} (**1**), fulleroid **2**, cyclopropane derivatives **3** and **4**, oxygen-bridged compound **5**, fullerene derivatives with four-membered-ring (**6**) and five-membered-ring (**7**), and noncyclic adduct **8** (Figure 1).

TABLE 2. Statistical Data of Experimental and Calculated ^{3}He Chemical Shifts at GIAO-HF/3-21G and GIAO-B3LYP/3-21G Levels for Compounds 1−8

	AM1		PM3	
	HF/3-21G	B3LYP/3-21G	HF/3-21G	B3LYP/3-21G
R[a]	0.98660	0.99301	0.98253	0.98807
SD[b]	0.21717	0.15706	0.24765	0.20492

[a] Regression coefficient. [b] Standard deviation.

The geometries of the endohedral fullerene compounds **1**−**8** were optimized only at semiempirical AM1 and PM3 levels because it was too time-consuming for the geometrical optimizations at higher levels such as HF and B3LYP. Helium-3 NMR chemical shifts of compounds **1**−**8** were computed at the GIAO-HF/3-21G and GIAO-B3LYP/3-21G levels with both AM1- and PM3-optimized structures. No great differences in the computation times for all four methods have been found. The calculated δ_{He} relative to the free ^{3}He along with the experimental δ_{He} in ppm are listed in Table 1 (Supporting Information).

From Table 1, it can be seen that the calculated δ_{He} by the GIAO-HF/3-21G method for both AM1- and PM3-optimized geometries relative to the experimental data tend to overestimate the chemical shifts by about 2−3 ppm, while those by GIAO-B3LYP/3-21G underestimate the chemical shifts by about 3−4 ppm. However, excellent linear relationships between the calculated ^{3}He NMR chemical shifts (δ_{cal}) and the experimental ^{3}He NMR chemical shifts (δ_{exp}) have been found for all four calculation methods (Figures 2−5, Supporting Information).

The statistical data for δ_{exp} and δ_{cal} calculated at GIAO-HF/3-21G and GIAO-B3LYP/3-21G levels with both AM1 and PM3 geometries are listed in Table 2. From Table 2,

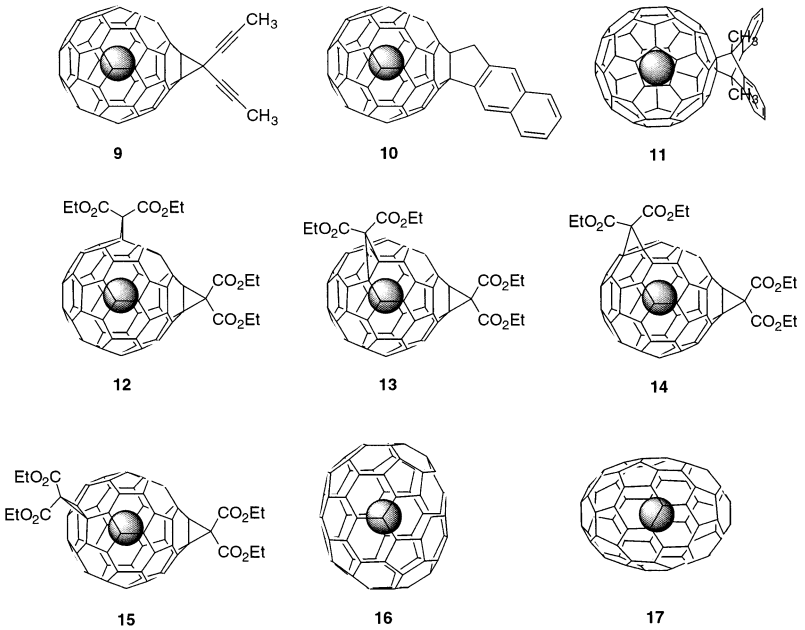

FIGURE 6. Structures of ^{3}He-encapsulated fullerene compounds **9**−**17**.

TABLE 3. Calculated, Corrected, and Experimental ^{3}He NMR Chemical Shifts and Statistical Data for Compounds 1−17

	B3LYP/3-21G//AM1		B3LYP/3-21G//PM3		
compd	δ_{cal}	δ_{corr}	δ_{cal}	δ_{corr}	δ_{exp}
1	−3.68	−6.06	−3.22	−5.85	−6.30[a]
2	−3.87	−6.32	−3.48	−6.19	−6.63[b]
3	−5.26	−8.20	−4.97	−8.13	−8.11[b]
4	−5.19	−8.10	−5.01	−8.19	−8.06[b]
5	−5.10	−7.98	−4.80	−7.91	−8.24[b]
6	−5.83	−8.97	−5.53	−8.86	−9.11[b]
7	−6.00	−9.20	−5.95	−9.41	−9.45[b]
8	−6.17	−9.43	−5.87	−9.31	−9.66[b]
9	−5.38	−8.36	−5.14	−8.35	−8.38[b]
10	−5.87	−9.03	−5.57	−8.92	−9.23[b]
11	−6.43	−9.78	−6.12	−9.64	−9.77[c]
12	−6.96	−10.50	−6.96	−10.73	−9.84[d]
13	−5.79	−8.92	−5.62	−8.98	−8.89[d]
14	−6.90	−10.42	−6.89	−10.64	−9.68[d]
15	−6.32	−9.64	−6.22	−9.77	−9.14[d]
16	−20.47	−28.81	−20.56	−28.51	−28.80[a]
17	−12.69	−18.27	−13.03	−18.67	−18.72[e]
R	0.99802		0.99674		
SD	0.35108		0.45042		
mean error	0.25		0.32		
max error	0.74		0.96		

[a] Reference 6. [b] Reference 10. [c] Reference 25. [d] Reference 13. [e] Reference 9.

it is obvious that all four methods have good linear relationships between δ_{cal} and δ_{exp} with regression coefficients greater than 0.98. However, a detailed comparison of the regression coefficient and standard deviation shows that the GIAO-B3LYP/3-21G method gives better linear correlations between δ_{cal} and δ_{exp} than does the GIAO-HF/3-21G method for both AM1 and PM3 geometries.

The Influence of Geometrical Optimization. On the basis of the results calculated at the GIAO-HF/3-21G and GIAO-B3LYP/3-21G levels, the latter method was chosen for the ^{3}He NMR chemical shift calculations. To compare the influence of the geometrical optimization on the δ_{cal} calculation, more fullerene compounds are included. These ^{3}He-encapsulated fullerene compounds are monoadducts of C_{60} with three-membered-ring (**9**), five-membered-ring (**10**), and six-membered-ring (**11**); *e* isomer (**12**), *trans*-4 isomer (**13**), *trans*-3 isomer (**14**), and *trans*-2 isomer (**15**) of Bingel bis-adducts of C_{60}; higher fullerenes C_{70} (**16**) and C_{76}-D_2 (**17**) (Figure 6).

Compounds **9**−**17** were optimized at both AM1 and PM3 levels. Then ^{3}He NMR chemical shifts of compounds **9**−**17** were computed by both GIAO-B3LYP/3-21G//AM1 and GIAO-B3LYP/3-21G//PM3 methods. Linear regression fittings of the δ_{exp} data and the δ_{cal} data obtained by GIAO-B3LYP/3-21G//AM1 and GIAO-B3LYP/3-21G//PM3 for compounds **1**−**17** are shown in Figures 7 and 8. Both fittings have very good linear correlations with regression coefficients greater than 0.997.

From the linear regression fittings, corrected chemical shifts (δ_{corr}) can be obtained from the corresponding

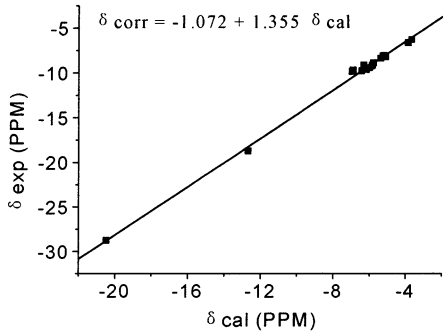

FIGURE 7. Linear regression fitting of δ_{exp} and δ_{cal} by B3LYP/3-21G//AM1 for compounds **1**−**17**.

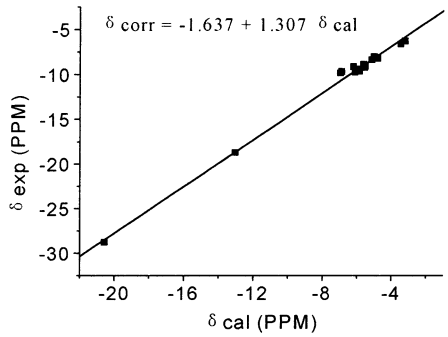

FIGURE 8. Linear regression fitting of δ_{exp} and δ_{cal} by B3LYP/3-21G//PM3 for compounds **1**−**17**.

correlation equations shown in Figures 7 and 8. The δ_{cal} along with the δ_{corr}, δ_{exp}, and statistical data are listed in Table 3.

It has been shown that the geometries of the host fullerene skeletons, in particular the extent of bond alternation in ^{3}He@C_{60}, sensitively affect the computed endohedral chemical shifts.[30−32] In our case, the δ_{cal} data for both AM1- and PM3-optimized geometries are quite close. This phenomenon is probably due to the fact that the geometrical parameters calculated at the AM1 and PM3 levels for ^{3}He@C_n and their derivatives have already approached the ideal geometrical parameters. By comparing the differences between the δ_{cal} data and the δ_{exp} data, the regression coefficient, the standard deviation, the mean error, and the maximum error in Table 3, we conclude that GIAO-B3LYP/3-21G//AM1 is a better method for calculating the ^{3}He NMR chemical shifts of ^{3}He@C_n and their derivatives. It is also noted that the largest errors are found for bis-adducts **12**, **14**, and **15**, where the calculated values are larger than the experimental values.

The Correction Equation. After the GIAO-B3LYP/3-21G//AM1 method is selected, a correlation equation derived from the δ_{cal} data and the δ_{exp} data of as many representative ^{3}He-encapsulated fullerene compounds as possible has to be derived in order to obtain an accurate and reliable δ_{corr} value from the δ_{cal} of a given fullerene

TABLE 4. Calculated and Experimental ^{3}He NMR Chemical Shifts of Compounds 18−27

compd	**18**	**19**	**20**	**21**	**22**	**23**	**24**	**25**	**26**	**27**
δ_{cal}	−11.08	−11.47	−11.90	−19.63	−18.63	−12.47	−12.19	−19.59	−20.05	−18.32
δ_{exp}	−15.31[a]	−16.35[a]	−16.45[b]	−27.18[a]	−25.33[a]	−17.84[a]	−17.17[a]	−27.46[c]	−28.14[c]	−25.56[c]

[a] Reference 24. [b] Reference 15. [c] Reference 8.

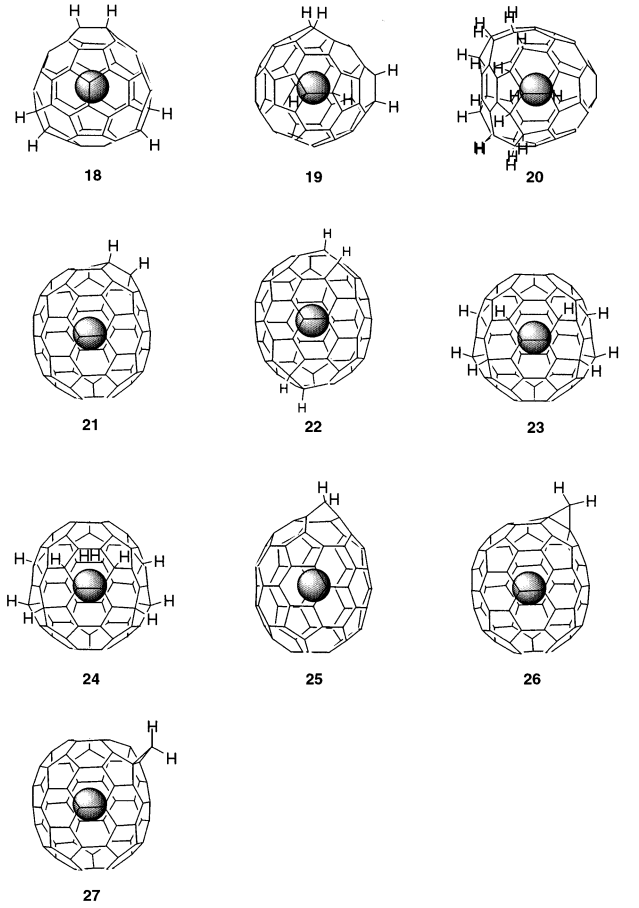

FIGURE 9. Structures of ^{3}He-encapsulated fullerene compounds **18**−**27**.

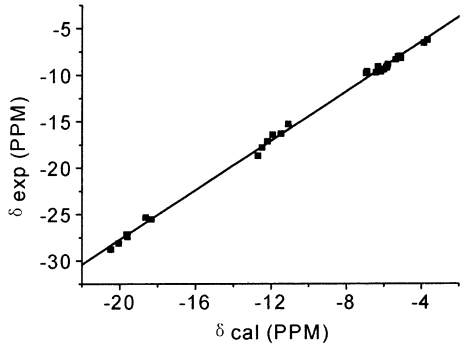

FIGURE 10. Linear regression fitting of δ_{exp} and δ_{cal} by B3LYP/3-21G//AM1 for compounds **1**−**27**.

compound. Therefore, ^{3}He@$C_{60}H_6$ isomers (**18**, **19**), ^{3}He@$C_{60}H_{18}$ (**20**), ^{3}He@$C_{70}H_2$ (**21**), ^{3}He@$C_{70}H_4$ major (**22**), ^{3}He@$C_{70}H_8$ (**23**), ^{3}He@$C_{70}H_{10}$ (**24**), and ^{3}He@$C_{70}(CH_2)$ isomers (**25**−**27**) (Figure 9) are added to include various kinds of ^{3}He-encapsulated fullerene compounds.

The δ_{cal} data calculated by GIAO-B3LYP/3-21G//AM1 along with the δ_{exp} data of compounds **18**−**23** are listed in Table 4.

TABLE 5. Experimental and Calculated Data of the Compounds 28−31

compd	28	29	30	31
δ_{cal}	−5.87	−6.07	−5.93	−6.00
δ_{corr}	−8.97	−9.24	−9.05	−9.15
δ_{exp}[a]	−9.28	−9.34	−9.21	−9.29

[a] Reference 12.

Linear regression fitting of the δ_{cal} data obtained by GIAO-B3LYP/3-21G//AM1 with δ_{exp} data for compounds **1**−**27** (Figure 10) yields an excellent correlation with a regression coefficient of 0.9989 and a SD of 0.36659. The correlation equation derived from the above linear regression fitting is

$$\delta_{corr} = -1.167 + 1.330\delta_{cal} \quad (1)$$

Isomer Differentiation of Monoadducts of [60]-Fullerene. To test the validity of correction eq 1, two pairs of *trans* and *cis* isomers of fullerene derivatives (**28**, **29** and **30**, **31**) (Figure 11)[12] having chiral centers were chosen. The δ_{cal} data computed by GIAO-B3LYP/3-21G//AM1 along with the δ_{corr} and δ_{exp} data for compounds **28**−**31** are listed in Table 5.

It can be seen from Table 5 that the δ_{corr} values match the δ_{exp} values very well within 0.3 ppm for the two pairs of *trans* and *cis* isomers of fullerene derivatives **28**−**31**. Furthermore, the δ_{corr} data indicate which isomer is more upfield shifted for each pair of isomers, which is fully consistent with the experimental results.

Applications

Assignment of [78]Fullerene Isomers. The δ_{cal} values for C_{2v}-C_{78} (**32**), $C_{2v'}$-C_{78} (**33**), and D_3-C_{78} (**34**) isomers (Figure 12) obtained by GIAO-B3LYP/3-21G//AM1 are −11.48, −11.42, −7.07 ppm, respectively. After corrections with eq 1, the corresponding δ_{corr} data are −16.44, −16.36, and −10.57 ppm, which are close to the experimental chemical shifts of −16.90, −16.78, and −11.93 ppm. These data confirm the previous assignments for these isomers based on the relative abundance of each isomer in the ^{13}C NMR spectrum of C_{78}.[9]

Assignment and Reassignment of [60]Fullerene Bis-adducts. There are at most eight positional isomers for the bis-adducts of C_{60} if the second addend is the same as the first one (Figure 13). Even though the mixture of and/or the individual isomers of ^{3}He@$C_{60}H_4$,[13,14] ^{3}He@C_{60}-$(C_3H_7N)_2$ (*N*-methylfulleropyrrolidines, Prato bis-adducts),[13] and ^{3}He@$C_{60}(C(CO_2Et)_2)_2$ (di(ethoxycarbonyl)-methanofullerenes, Bingel bis-adducts)[13] have been separated and their ^{3}He NMR spectra have been recorded, some ^{3}He NMR peaks need assignments and reassignments.

Table 6 lists the ^{3}He δ_{corr} data obtained from using eq 1 for which the δ_{cal} data were calculated by GIAO-B3LYP/

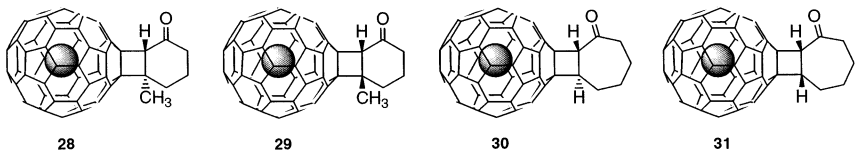

FIGURE 11. Structures of ^{3}He-encapsulated fullerene compounds **28**−**31**.

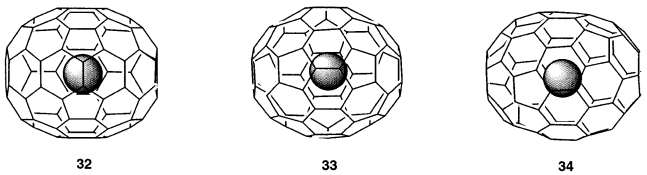

FIGURE 12. Structures of ^{3}He-encapsulated fullerene compounds **32**−**34**.

3-21G//AM1 for all eight isomers of ^{3}He@$C_{60}H_4$, ^{3}He@C_{60}-$(C_3H_7N)_2$, and ^{3}He@$C_{60}(C(CO_2Et)_2)_2$, along with the corresponding monoadducts.

From the computed δ_{corr} data in Table 6, we can see that (1) the *trans*-1 isomer is the most downfield shifted among the eight bis-adduct isomers, and it is even more downfield shifted than the corresponding monoadduct for the unstrained cyclic (Prato product) and noncyclic ($C_{60}H_n$) fullerene compounds; (2) the general trend of the ^{3}He NMR chemical shifts for the bis-adducts of the first two series is *trans*-1 > *cis*-3 > *trans*-4 > *trans*-2 > *cis*-1 > *e* ≈ *trans*-3 > *cis*-2, while the order for the *trans*-2 and *cis*-1 isomers of the Bingel bis-adducts is reversed.

The ^{3}He NMR spectra of the ^{3}He@$C_{60}H_4$ isomers have been measured before.[13,14] However, no assignments of the ^{3}He NMR peaks were made except for the *cis*-1 isomer.[14] The computed δ_{corr} values of the eight isomers of ^{3}He@$C_{60}H_4$ are −8.47 (*trans*-1), −9.47 (*cis*-3), −9.68 (*trans*-4), −10.97 (*trans*-2), −11.38 (*cis*-1), −12.64 (*e*), −12.65 (*trans*-3), −13.06 (*cis*-2) ppm. After correlations with the calculated δ_{corr} data, the δ_{exp} at −10.30, −11.26, −11.56, −12.75, and −12.79 ppm in the ^{3}He NMR spectrum of ^{3}He@$C_{60}H_4$ isomers (Figure 5 of the Supporting Information in ref 13) can be tentatively assigned as *trans*-4, *trans*-2, *cis*-1, *e*, and *trans*-3 isomers, respectively. The much weaker peaks at −10.81 and −12.86 ppm in the spectrum are probably due to noise. Meanwhile, the δ_{exp} at −10.0, −10.9, −12.42, and −12.48 ppm in the ^{3}He NMR spectrum of the five ^{3}He@$C_{60}H_4$ isomers (Figure 14, cf. Figure 4 in ref 14) match nicely with δ_{corr} of *trans*-4, *trans*-2, *e*, and *trans*-3 isomers. Note that the different δ_{exp} data in the two ^{3}He NMR spectra of ^{3}He@$C_{60}H_4$ are due to the different solvents used in the measurements. The obtained δ_{corr} (−8.47 ppm) of the *trans*-1 isomer is the only one among the eight isomers of ^{3}He@$C_{60}H_4$ more downfield shifted than that (−9.37 ppm) of ^{3}He@$C_{60}H_2$. The existence of the *trans*-1 isomer was observed in the ^{1}H NMR spectrum of the $C_{60}H_4$ isomers.[14] Therefore, the peak at −9.3 ppm in Figure 14 can be undoubtedly assigned to the *trans*-1 isomer.

The ^{3}He NMR spectrum (Figure 15, cf. Figure 3 in ref 13) of the Prato reaction mixture containing mono-, bis-, and tris-adducts has been reported.[13] Four bis-adduct isomers have been isolated and measured by ^{3}He NMR spectra. The peaks at −10.14, −10.92, −12.33, and −12.36 ppm were assigned as *trans*-4, *trans*-2, *cis*-3, and *trans*-3 isomers, respectively.

The δ_{corr} values for the *e* (−12.18 ppm) and *trans*-3 (−12.19 ppm) isomers are almost the same, just as the experimental overlapping peaks at −12.33 and −12.36 ppm are also very close. The peak at −12.33 ppm should be reassigned as the *e* isomer instead of as the previously assigned *cis*-3 isomer.[13] In fact, the calculated δ_{corr} (−9.65 ppm) of the *cis*-3 isomer is much more downfield shifted than that of the *e* and *trans*-3 isomers. Our reassignment is verified by the corrections[50] of the previous assignments of Prato bis-adducts of C_{60}.[51] One major isomer of the Prato bis-adducts of C_{60}, previouly assigned as the *cis*-3 isomer,[51] was later identified as the *e* isomer.[50] Prato and co-workers further revealed that the *cis*-2 isomer is also a major isomer of the Prato bis-adduct with amounts comparable with the *trans*-4 isomer, and the *trans*-1 isomer has the least amounts among the six isolated bis-adduct isomers from the reaction of C_{60} with paraformaldehyde and *N*-methylglycine.[50] The computed δ_{corr} of the *cis*-2 isomer is the most upfield shifted among the Prato bis-adducts. Judging by the calculated δ_{corr} values and relative ^{3}He NMR peak intensities in Figure 15, the peak at ca. −12.8 ppm is now assigned as the *cis*-2 isomer. The peak at ca. −8.8 ppm, which is even more downfield shifted than that of the Prato monoadduct, is assigned as the *trans*-1 isomer of the Prato bis-adducts,

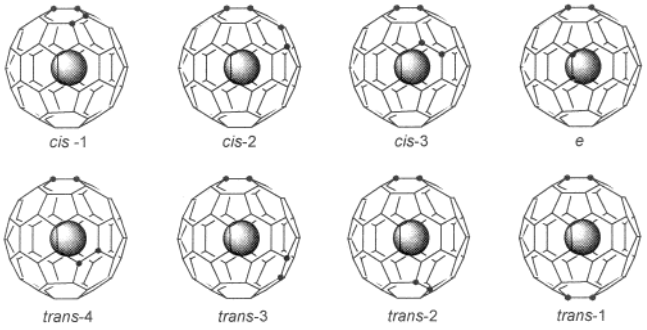

FIGURE 13. Structures of eight positional isomers of ^{3}He-encapsulated bis-adducts of C_{60}.

TABLE 6. Computed ^{3}He δ_{corr} by GIAO-B3LYP/3-21G//AM1 for ^{3}He@$C_{60}H_4$, ^{3}He@$C_{60}(C_3H_7N)_2$, and ^{3}He@$C_{60}((C(CO_2Et)_2)_2$ along with Corresponding Monoadducts

	bis-adduct								
Series	*trans*−1	*trans*−2	*trans*−3	*trans*−4	*e*	*cis*−3	*cis*−2	*cis*−1	Mono-adduct
$C_{60}H_n$	−8.47	−10.97	−12.65	−9.68	−12.64	−9.47	−13.06	−11.38	−9.37
Prato	−8.85	−10.74	−12.19	−9.75	−12.18	−9.65	−12.38	−10.84	−9.15
Bingel	−8.46	−9.57	−10.34	−8.87	−10.42	−8.84	−10.56	−9.48	−8.07

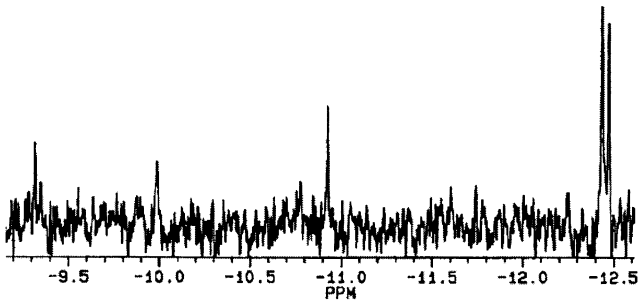

FIGURE 14. ^{3}He NMR spectrum of five ^{3}He@$C_{60}H_4$ isomers. Reprinted with permission from ref 14. Copyright 1997 Elsevier.

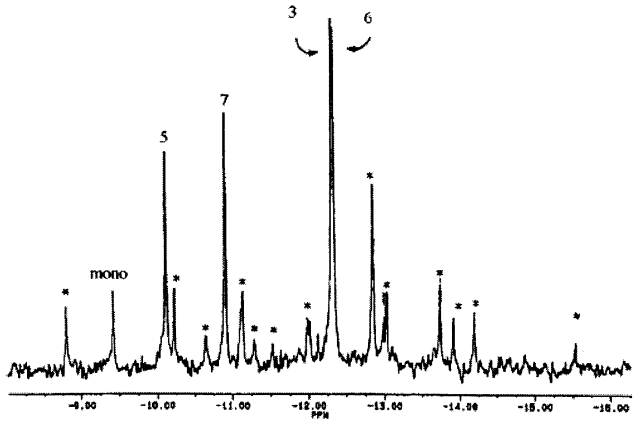

FIGURE 15. ^{3}He NMR spectrum of the Prato reaction mixture containing mono-, bis- and tris-adducts. Reprinted with permission from ref 13. Copyright 1996 American Chemical Society.

consistent with the calculated δ_{corr} results of the monoadduct and the *trans*-1 isomer. It should be noted that the ^{3}He NMR patterns for the *trans*-1, *trans*-4, *trans*-2, *e*, and *trans*-3 isomers of the ^{3}He@$C_{60}H_4$ and the Prato bis-adducts are quite similar.

On the basis of the calculated δ_{corr} values of −10.56 and −8.84 ppm for the *cis*-2 and *cis*-3 isomers of the Bingel bis-adducts of C_{60}, it seems that the peak at −10.2 ppm in ref 13 should be assigned as the *cis*-2 isomer instead of the *cis*-3 isomer, similar to the case of the Prato bis-adducts. This assignment is further supported by the similar UV−vis spectra of the assumed *cis*-3 isomer[13,51] of the Bingel bis-adducts and that of the *cis*-2 isomer of the Prato bis-adducts.[50]

Conclusions

The work reported in this paper establishes the feasibility of GIAO-HF/3-21G and GIAO-B3LYP/3-21 with both AM1- and PM3-optimized structures for the ^{3}He NMR chemical shifts of ^{3}He-encapsulated fullerenes and fullerene derivatives. Very good linear relationships between computed and experimental ^{3}He NMR chemical shifts of ^{3}He-encapsulated compounds have been determined. Among the four calculation methods, GIAO-B3LYP/3-21G//AM1 gives the best results. The corrected ^{3}He NMR chemical shifts developed in this paper can be utilized to obtain accurate theoretical ^{3}He NMR chemical shifts and applied to structural assignments and reassignments of ^{3}He-encapsulated fullerenes and fullerene derivatives.

Acknowledgment. This work is partly supported by the "Hundred Talents Program" of the Chinese Academy of Sciences and the National Science Fund for Distinguished Young Scholars (20125205).

Supporting Information Available: Calculated and experimental ^{3}He NMR chemical shifts for compounds **1**−**8** (Table 1), linear regression fittings of δ_{exp} and δ_{cal} by HF/3-21G//AM1 (Figure 2), B3LYP/3-21G//AM1 (Figure 3), HF/3-21G//PM3 (Figure 4), and B3LYP/3-21G//PM3 (Figure 5) for compounds **1**−**8**. This material is available free of charge via the Internet at http://pubs.acs.org.

JO0341259

(50) Kordatos, K.; Bosi, S.; Da Ros, T.; Zambon, A.; Luccini, V., Prato, M. *J. Org. Chem.* **2001**, *66*, 2802−2808.
(51) Lu, Q.; Schuster, D. I.; Wilson, S. R. *J. Org. Chem.* **1996**, *61*, 4764−4768.